Synthesis and Characterization of Ulvan-Alginate Hydrogel Beads as a Scaffold for Probiotic Immobilization

Wahyu Ramadhan[1,2*]*, Fadya Aliciya* Ramadhani[1]*, Devani* Sevica[1]*, Safrina Dyah* Hardiningtyas[1], and *Desniar*[1].

[1]Department of Aquatic Product Technology, Faculty of Fisheries and Marine Sciences, IPB University, Bogor, West Java, 16680, Indonesia
[2]Center of Coastal and Marine Resources Studies (PKSPL), IPB University, Bogor, 16127, Indonesia

Abstract. Probiotic drinks have various benefits for the digestive tract. However, there is a problem with ensuring the viability of probiotics and their functionality while passing through the digestive tract to the large intestine, thus an alternative strategy is needed to maintain the viability of probiotics, namely hydrogel encapsulation of natural biopolymers such as ulvan and alginate. Hydrogels constructed from ulvan and alginate were predicted to be suitable for the challenge as a probiotic bioreactor that could stimulate human digestive health because its porosity and retention capacity could be chemically controlled. The aims of the study were to evaluate the characteristics of the selected ulvan concentrations and to determine the resistance of encapsulated probiotic bacteria in simulated gastric fluid (SGF) and simulated intestinal fluid (SIF). The research involved characterizing the hydrogel using different concentrations of ulvan (1%, 2%, 3%, and 4%) along with 2% alginate. Ulvan-alginate hydrogel produced the highest gel fraction and swelling ratio of 98.8% and 19.7%. The hydrogel system composed of 1% ulvan and 2% alginate effectively preserved the viability of probiotic bacteria in both SGF and SIF environments, with survival rates of 3.41×10^7 and 0.14×10^7 log CFU/g, respectively.

1   Introduction

Probiotic bacteria that are present in sufficient quantities strengthened the immune system of the body and increased the nutritional content of food [1–5]. The importance of probiotics to human health affected people's willingness to consume probiotic-containing products. Probiotics were commonly found in food products with a minimum standard of probiotic bacterial content in food of 10^6-10^7 colony-forming unit (CFU)/g [6]. However, there are concerns regarding the viability and functionality of probiotics as they passed through the human digestive tract until they reached the large intestine in significant numbers [7–9]. In addition to the minimum probiotic concentration, it is crucial to take into account other factors when formulating probiotics in food materials, including resistance to pH, oxygen, and temperature [10]. As a result, probiotic bacteria have to be carefully monitored for their

---

* Corresponding author: wahyu.ramadhan@apps.ipb.ac.id

survival and functionality as they can rapidly lose viability [11]. This implies that probiotic bacteria are sensitive to the external environment. Encapsulation is a strategy that could be employed to sustain the presence of probiotic bacteria.

Researchers extensively studied encapsulation technology to protect bacteria during processing, transportation, storage, and passage through the human digestive system [1–3,12]. Encapsulation systems were commonly developed based on proteins, biopolymers, and lipids [10]. However, in recent years, protein-based encapsulation technology derived from animal sources received negative responses, particularly from vegan and Muslim groups who raised concerns about halal issues. Encapsulation based on lipids, fats, oils, waxes, and other biopolymers could also be used as a delivery system [13]. However, these biopolymers were not suitable for probiotic encapsulation as they could not withstand the gastric fluid in the stomach [14–18]. Because of their outstanding biocompatibility, biodegradability, and minimal immunogenicity, polysaccharides-based encapsulation materials were generally regarded as the best scaffold for the administration of small compounds, bioactive substances, and therapeutic cells [19].

Materials known as hydrogels were specifically designed to encase biological components. They provide an environment in which most biological molecules can thrive due to their high-water content [20–23]. Their crosslinked structure also made them a perfect material for shielding encapsulated biological components from immune detection or degradation. This made them desirable for regulated medication administration and the encapsulation of bacteria or cells with potential therapeutic uses [22,24,25]. Biopolymer-based hydrogels demonstrated superior performance in the encapsulation of active ingredints [26]. One popular natural biopolymer used for encapsulation was alginate, which was a polysaccharide derived from brown seaweed extract. Alginate had garnered significant attention due to its excellent physicochemical and mechanical properties, including a simple structure, easy availability of raw materials, low toxicity, gentle processing, ease of gel matrix formation, as well as biocompatibility, versatility, acid resistance, non-toxicity, and ease of handling [27]. Alginate had been widely used in hydrogel fabrication in various fields, particularly in biomedicine. However, despite its favorable characteristics, alginate had limitations, such as brittleness, heat instability, precipitation at low pH, and metal incompatibility [28]. The utilization of 2% alginate concentration represents the optimum concentration for hydrogel fabrication, as it facilitates the formation of morphology and enhances the mechanical strength of the resultant hydrogel [29–31]. Despite of alginate has been extensively employed as a scaffold, particularly for encapsulating nutritional components, its adhesive properties are limited when it approaches to encapsulating living entities or bacteria. To date, alginate needs an additional biopolymer to enhance encapsulation efficiency and regulate the release of biological milieu. Another potential biopolymer was ulvan, which exhibited a unique structure capable of generating functional hydrogels.

Ulvan was a sulfated polysaccharide derived from green seaweed, particularly *Ulva* species [32–34]. Recent research had presented a systematic report on the generation of ulvan hydrogel using different systems [35]. However, the synthesis of alginate-ulvan-based hydrogels, particularly in the field of food and as a probiotic vehicle delivery system, had not been reported thus far. Theoretically, the functionality of probiotics in the digestive system could be enhanced by employing specific probiotics strain in hydrogel beads. Moreover, ulvan and alginate polymers were predicted to enable control over their porosity and retention capacity. Nevertheless, the appropriate ratio of alginate and ulvan to produce high-quality hydrogels remained unclear. To the best of the author's knowledge, there is only one publication documenting the combination of Ulvan and Alginate in a single system [31]. However, this report focused on the application of this system in exfoliating cosmetic products rather than as a food encapsulation system. To date, this study aimed to evaluate

and investigate the synthesis of alginate-ulvan hydrogel beads, as well as their gel properties and ability to protect probiotics during simulated digestive conditions. Eventually, hydrogels fabricated from ulvan and alginate polymers held promising potential as probiotic bioreactors and scalable scaffolds, capable of promoting human digestive health.

2 Materials and Methods

2.1 Materials

The ulvan utilized in this investigation was extracted from *Ulva lactuca* seaweed collected from Ujung Genteng, Sukabumi, West Java, Indonesia. The Alginic acid used was obtained from HIMEDIA. Other materials employed included $CaCl_2$ (Merck), Man Rogosa Sharpe Agar (MRSA, Merck), Man Rogosa Sharpe Broth (MRSB, Merck), *Lactobacillus plantarum* FNCC 0020 bacteria, NaCl (Merck), NaOH (Merck), pepsin, and physiological saline solution. The equipment used in this study comprised an analytical balance, petri dishes, magnetic stirrer, magnetic bar, syringe, centrifuge, autoclave, incubator, micropipette (DragonLab, Beijing 101318, China), rheometer (TA Instrument DHR1), colony counter, and glassware (Pyrex).

2.2 The fabrication of Ulvan-Alginate (ULV-ALG) Hydrogel

First, ulvan was extracted from *Ulva lactuca* seaweed following the methodology described in our previous report [34]. The extracted ulvan was subsequently evaluated for its yield, sulfate content, viscosity, moisture content, molecular weight, and functional groups using FT-IR spectroscopy. The extracted ulvan was dried before being used for hydrogel synthesis and diluted in various concentrations (1%, 2%, 3%, and 4% w/v). Alginate was prepared as a fixed solution (2% w/v).

The fabrication of the Ulvan-Alginate (ULV-ALG) hydrogel scaffold was performed using the extrusion or dropping method. A 20 mL syringe was employed, and a calcium chloride ($CaCl_2$) solution was used as the gel precursor. The process began by preparing ulvan solutions with concentrations of 1%, 2%, 3%, and 4% (w/v), along with a 2% sodium alginate solution. These solutions were then mixed in a 1:1 ratio and dropped into a 3% (w/v) $CaCl_2$ solution while stirring at 250 rpm using a magnetic stirrer. Hydrogel beads were formed at the bottom of the $CaCl_2$ solution. Subsequently, rinsing, filtration, and drying steps were performed. The resulting hydrogel beads were stored at 4°C for 2 hours. The hydrogel beads generated with different concentrations were labeled as ULV-ALG-a (ulvan 1%, alginate 2%), ULV-ALG-b (ulvan 2%, alginate 2%), ULV-ALG-c (ulvan 3%, alginate 2%), and ULV-ALG-d (ulvan 4%, alginate 2%).

The hydrogel appearance, gel fraction, swelling ratio, and rheology of the generated ULV-ALG hydrogels from each formulation were examined. These analyses were conducted to identify the preferred hydrogel based on the gel fraction and swelling ratio values. The selected concentration of the hydrogel precursor was then utilized to immobilize the probiotic bacteria. The incorporation of probiotic bacteria was achieved by adding a total volume of 2.5 mL ($\sim 1.0 \times 10^9$) of *Lactobacillus plantarum* to the ULV-ALG (2.5 mL total precursor solution) before the gelation process in the $CaCl_2$ solution. The bacteria were safely immobilized within the gel system of ULV-ALG beads, which were subsequently subjected to simulated gastric fluid (SGF) and simulated intestinal fluid (SIF) analyses to evaluate the ability of the ULV-ALG hydrogel as an immobilization scaffold for probiotics in gastrointestinal gut simulation.

2.2 The evaluation of ULV-ALG hydrogel properties

2.2.1 Gel Content

Gel fraction or gel content was performed by preparing ULV-ALG hydrogel samples from each treatment and initially weighing them for dry weight (Wp). This process was carried out following the slight modification [20]. Subsequently, the hydrogels were incubated for 48 hours at a temperature of 37°C. The dried hydrogels were then reweighed (Wd) to calculâtes the percentage of gel fraction. The calculation for the gel fraction was as follows:

$$Gel\ Content\ (\%) = \frac{Wd}{Wp} \times 100\% \qquad (1)$$

Wp = the Initial dry weight of the gel, and

Wd = Final dry weight of the gel

2.2.2 Swelling Ratio

Swelling testing of hydrogel aimed to assess its absorption capacity during the swelling process. The testing procedure was modified based on Zhao [36]. The test involved immersing ULV-ALG hydrogel beads in 1 mL of water for 30 days to induce swelling, with observations made on days 1, 10, 20, and 30. Subsequently, the samples were filtered for a few minutes and dried using tissue paper. The calculation of the swelling ratio for each hydrogel was as follows:

$$Swelling\ ratio\ (\%) = \frac{(w - w0)}{w0} \times 100\% \qquad (2)$$

w = the Mass of gel after swelling and

w0 = the mass of dry gel.

2.2.3 Rheology

Rheological analysis of the ULV-ALG hydrogel was conducted using an MCR 302 rheometer (Anton Paar, Graz, Austria) equipped with a 25 mm diameter conical plate in oscillation mode (EMS/TEK 500 disposable plate). The hydrogel solution was placed on the rheometer stage and incubated at 37°C for 6 hours. The angular frequency was set to range from 1 to 100 (rad/s). The measurement was continued until the equilibrium storage modulus (G') and loss modulus (G") were reached, as described by [22].

2.2.4 Biologycal Test - Total Probiotic Bacteria Test

The evaluation of total probiotic bacteria was conducted by modifying the procedures listed in AOAC [37]. *Lactobacillus plantarum* were harvested by culturing on MRSA medium and incubated at 37 °C for 48 hours, then harvested on MRSB medium and incubated at 37°C for 24 hours. Bacteria growing on MRSB media were then centrifuged at 3000 rpm for 15 minutes at 20°C. The results of centrifugation obtained the supernatant and pellet, and the supernatant was removed using a pipette, and the pellet obtained was added with half the volume of sterile water used previously.

The harvested bacteria were then immobilized on the hydrogel sample. A total of 1 g of the hydrogel sample was homogenized and dissolved in 9 mL of physiological saline until a 10^{-1} dilution was obtained. The solution was pipetted as much as 1 mL and put into the first test tube containing 9 mL of physiological saline to obtain a 10^{-2} dilution. Dilution was continued until 10^{-8} dilution. This dilution was performed to facilitate easy and precise counting. At this specific level of dilution, the number of colonies counted is sufficiently high to ensure statistical accuracy, yet low enough to avoid errors caused by colony overlap. The last four dilutions were pipetted as much as 1 mL and transferred to a sterile petri dish. Each sterile petri dish was then added with MRSA media and shaken until the surface was evenly distributed and left for a few moments to harden. The petri dish was then placed in an incubator at 37 °C for 48 hours. Observations were made by counting the number of bacterial colonies contained in a petri dish with a colony counter. The number of colonies that could be counted was a petri dish that had bacterial colonies ranging from 25–250 colonies. The calculation of the number of colonies was as follows:

$$N = \frac{\sum C}{[(1 \times n1) + (0.1 \times n2)] \times (d)} \qquad (3)$$

N = the number of colonies, expressed in colonies per mL or colonies per g,
$\sum$C = number of colonies on all plates counted,
n1= the number of cups in the first retail is calculated,
n2 = the number of cups at the second retail is calculated, and
D = the first dilution counted.

2.2.5 Simulated Gastric Fluid Analysis

The analysis of simulated gastric fluid was conducted following the methodology outlined by Afzaal [38] with slight modifications. Both free and encapsulated ULV-ALG hydrogel beads were subjected to gastric fluid conditions. Gastric fluid was prepared by adding 3 g/L of pepsin to a sterile NaCl solution. The pH of the gastric juice was adjusted to a range of 1.8-2. Two grams of free and encapsulated ULV-ALG hydrogel beads were suspended in the prepared gastric fluid solution and incubated at 37 °C for 2 hours. To determine the number of viable bacteria, MRS agar was utilized, and the colony-forming units (cfu/g) were calculated. The survival of encapsulated probiotic bacteria was recorded at 0, 60, and 120-minute intervals.

2.2.6 Simulated Intestinal Fluid Analysis

Survival of probiotics in the gastrointestinal tract was crucial, especially following gastric conditions. The viability of both free and encapsulated probiotics was assessed, following a modified protocol based on Afzaal [38]. The tolerance of encapsulated bacteria to intestinal transit conditions was evaluated by immersing ULV-ALG hydrogel beads into a simulated intestinal solution. The simulated intestinal solution was prepared using 0.1 N NaOH solution sterilized to pH 8. ULV-ALG hydrogel granules that had been previously soaked in simulated gastric fluid (SGF) solution for 2 hours were placed into the prepared intestinal solution (simulated intestinal fluid, SIF), followed by incubation at 37°C. The number of bacteria was then counted by calculating colony-forming units (cfu/g). The survival of encapsulated probiotic bacteria was assessed at 60 and 120-minute intervals. The SGF and SIF analysis were conducted in a sterile and sanitary manner.

2.3 Data Analysis

The data collected for this study were evaluated using one-way analysis of variance (ANOVA), with 0.05 selected as the level of statistical significance. The data were

represented as mean SD of triplicates. After that, the Duncan Multiple Range Test was used to assess the significant data by using the SPSS 25.00 Statistical Analysis software.

3 Results and Discussions

3.1 Characterization of Ulvan extracted from *Ulva lactuca*

Ulva lactuca was a polymorphic species, displaying morphological variations dependent on the water salinity level or bacterial symbiosis, and exhibiting the capacity to grow both attached and free-floating in marine waters [39]. The appearance of *U. lactuca* was characterized by thin, smooth, undulating leaf-like structures with colors ranging from bright to dark green, and a dark-colored thallus (Figure 1A).
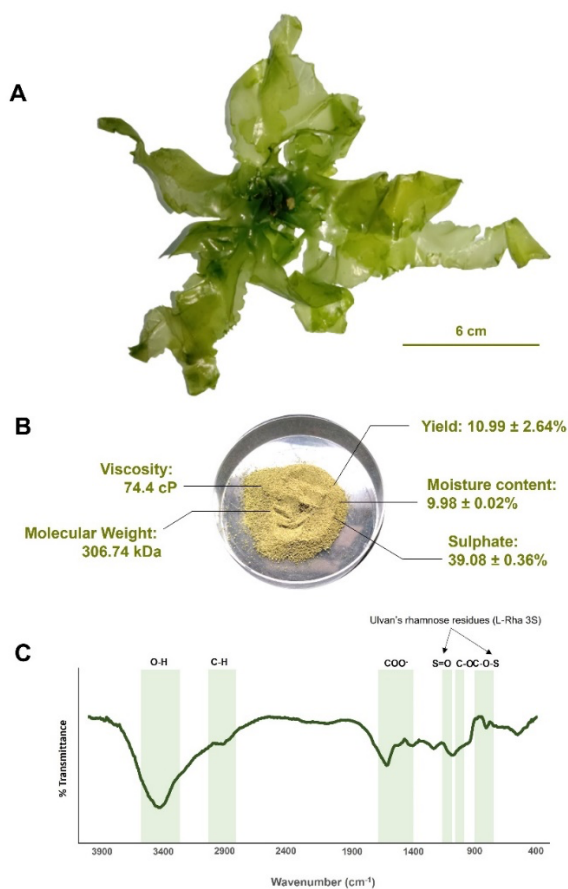

Fig. 1. A. Visualization of *Ulva Lactuca,* B. Ulvan powder and its chemical and physical properties, C. Functional group of uvan characterized by Fourier Transform Infra Red.

Figure 1B illustrated Ulvan powder and its corresponding chemical properties. The ulvan yield, a crucial factor in ulvan extraction, reached approximately 10.99% through the use of a combination of hot water extraction solvents, followed by alcohol precipitation and purification technique. The resulting molecular weight of ulvan ranged around 306.74 kDa.

This molecular weight aligned with the general findings of 100-500 kDa [32]. Molecular weight was closely associated with the viscosity value obtained (74.4 cP). Ulvan with higher molecular weights held promise as functional food fillers and supplements [40]. Furthermore, the sulfate content parameter was recorded to be 39.08%. This sulfate content was strongly linked to ulvan's functional properties as an antioxidant, anticoagulant, and its biological activities, as well as its potential as a hydrogel constituent. Figure 1C exhibited the results of functional group analysis through FTIR testing, indicating the prevalence of C-O-S functional groups as a primary marker of ulvan [34]. Additionally, C-O functional groups were observed in the absorption band range of 983 cm^{-1}, signifying the presence of C-O glycosidic bonds. The sulfate functional group was also evident at the absorption band of 1,215 cm^{-1}. Moreover, in the range of 1400-1600 cm^{-1}, stretching vibrations of O-C-O groups, characteristic of carboxyl and uronic acid groups in ulvan, were identified [41,42].

3.2 Visualization of ULV-ALG Hydrogel beads

The appearance of ULV-ALG hydrogel encompassed parameters such as the color and shape of the formed beads. The synthesis of ulvan-alginate hydrogel was carried out with a constant concentration of 2% alginate and varying concentrations of ulvan at 1%, 2%, 3%, and 4%. Visualizing the ulvan-alginate hydrogel revealed slight differences in color for each treatment (Figure 2).
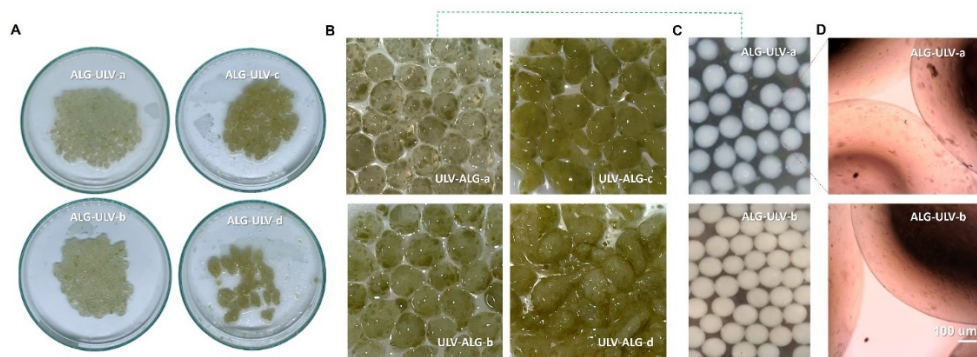

Fig 2. A. Visualization of ULV-ALG Hydrogel in petri dish and B. its magnification, C. Appearance of ULV-ALG Hydrogel and evaluation in aquades, C. Appearance of ULV-ALG Hydrogel and evaluation by Light Microscope (100x Mag.)

The observation results of the hydrogel appearance demonstrated the shape and color of each treatment. ULV-ALG-a and ULV-ALG-b treatments exhibited perfectly spherical shapes with a clear and slightly greenish color. The ULV-ALG-c treatment showcased imperfectly shaped beads with a green color, while the ULV-ALG-d treatment displayed irregularly shaped beads with a darker green color compared to the previous treatments. The distinct appearances of ULV-ALG hydrogel in each treatment were attributed to the high concentration of ulvan used. A high ulvan concentration profoundly impacted the shape, texture, and color of the hydrogel. Hydrogels with higher ulvan concentrations tended to have a firmer texture and higher gel strength. By increasing the concentration of ulvan in the hydrogel, the ulvan molecules are able to establish stronger connections with one another, resulting in the formation of a more compact and unified network [43]. In addition, the study conducted by Selvasudha [31] primarily investigated formulations with alginate concentrations ranging from 1.5% to 2% w/v, together with 2.5% $CaCl_2$. In line with our results, their research findings demonstrated the creation of spherical beads of 1000 μm in

size, with an encapsulation efficiency of 98%. The incorporation of sodium alginate with ulvan polysaccharide improves the ability of ulvan to form gels, making it easier to create stable, round microbeads.

3.3 Gel Content

Gel content was a commonly used parameter in testing the physical properties of synthesized hydrogels to assess the quantity of the raw materials employed in their production [44]. The gel fraction, or gel content, also indicated the presence of crosslinking within the hydrogel network. The obtained gel fraction percentage ranged from 97.2% to 98.8% (Figure 3). The research findings demonstrated that the formed hydrogels exhibited high stability across all formulations. ULV-ALG-b treatment achieved the highest gel fraction percentage at 98.8±0.15%, while ULV-ALG-d treatment obtained the lowest gel fraction percentage at 97.4±1.11%.
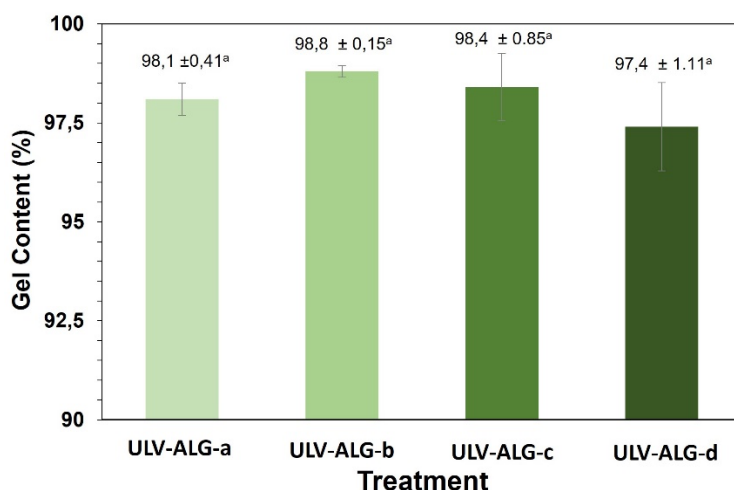

Fig. 3. Gel Content of ULV-ALG Hydrogel

Gel fractions above 50% indicated that the hydrogel possessed mechanical stability and good gel strength [45,46]. Hydrogels with high gel fractions (>90%) indicated a greater number of crosslinking bonds, resulting in a denser network with smaller intercrosslinking spaces. Conversely, hydrogels with low gel fractions exhibited fewer crosslinking bonds, leading to a more open network with larger intercrosslinking spaces. Importantly, all the ULV-ALG treatments demonstrated high gel content, indicating the successful synthesis of alginate and ulvan in the gel system, resulting in a compact and homogeneous gel fraction.

3.4 Swelling ratio

Swelling ratio was a measure of a polymer's ability to absorb water [22]. Based on Table 1, it could be observed that as the concentration of ulvan increased, the percentage of swelling ratio decreased.

Table 1 Swelling ratio of ULV-ALG hydrogel

Hydrogel system	Swelling ratio (%)			
	1-day	10-day	20-day	30-day
ULV-ALG-a	15.28 ± 2.13	13.79 ± 3.69	19.78 ± 9.22	4.91 ± 13.46
ULV-ALG-b	16.33 ± 2.45	7.11 ± 2.80	1.94 ± 2.18	-4.60 ± 3.30
ULV-ALG-c	12.75 ± 1.18	2.28 ± 0.53	1.02 ± 1.54	-4.93 ± 0.84
ULV-ALG-d	0.79 ± 1.91	-17.32 ± 15.35	-22.04 ± 14.35	-17.79 ± 15.84

The swelling ratio obtained on the first day showed that ULV-ALGa, b, and c exhibited similar swelling ratios, whereas ULV-ALGd showed the lowest swelling result. Interestingly, ULV-ALGd showed degradation after soaking from day 10 to 30, indicated by a negative value in its swelling ratio. In contrast, ULV-ALGa demonstrated more stable swelling performance up to day 30. Swelling ratio testing revealed that ULV-ALG-a achieved the highest value of 19.7% on the 20-day of immersion. The negative value of swelling ratio indicated that the hydrogel experienced degradation, possibly due to its composition of natural polymers.

3.4 Rheology

The rheological testing conducted included the measurement of storage modulus (G') or elastic modulus and loss modulus (G") or viscous modulus. The values of G' obtained for each sample showed an increase with the increment of angular frequency (rad/s). The G' values ranged from 2370 to 11080 (Pa) (Figure 4). ULV-ALG-a treatment obtained the highest value at 11080 (Pa), while ULV-ALG-b treatment obtained the lowest value at 2370 (Pa). Loss modulus or viscous modulus (G") represented the measure of energy dissipated in a material after forming a system such as a gel and was inversely proportional to the storage modulus (G') [47].
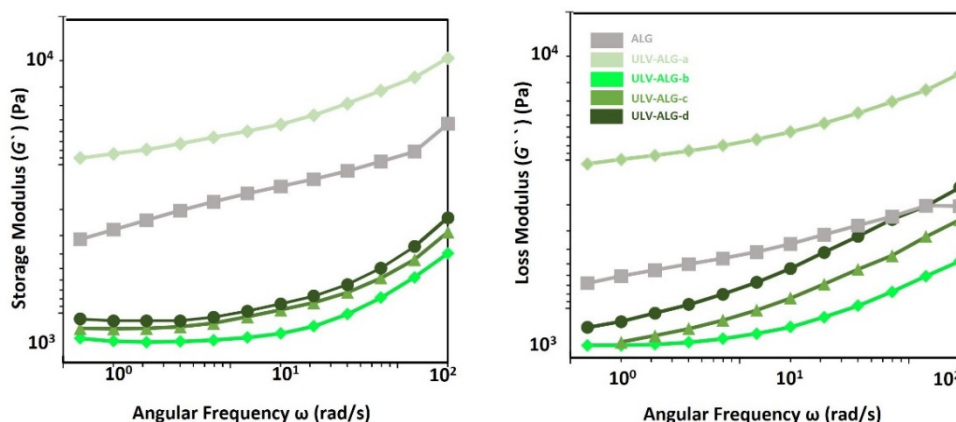

Fig. 4. Rheology profile of ULV-ALG hydrogel

The values of G'' at angular frequencies of 1-100 rad/s ranged from 2140 to 9345 (Pa). ULV-ALG-a treatment yielded the highest value at 9345 (Pa), while ULV-ALG-b treatment produced the lowest value at 2140 (Pa). The notable difference in values between ULV-ALG-b and other formulations indicated the influence of ulvan addition in the formed hydrogel system. The obtained values of G' and G'' for each hydrogel formulation were

closely related, indicating the strength of the formed gel and the energy dissipation or deformability. Overall, the G' values for all hydrogel formulations were higher than the G'' values. High G' values indicated that the polymer was stable during gelation, resulting in a more robust structure. The suitable polymers for forming 3D matrices like hydrogels should exhibit a balance between elastic modulus and viscous modulus [47]. Despite slight differences in the Young's modulus values produced, the variations in ulvan concentration resulted in an elasticity range remaining below 10,000 Pa. Interestingly, the stiffness and elasticity of the hydrogel can be categorized between conventional (relatively hard) gels and ultrasoft gels. Ultrasoft hydrogels facilitate a dynamic interaction between bacteria and the hydrogel, owing to the 3D microenvironment of the hydrogel that allows bacterial penetration through its porous network [48].

3.5 Probiotic survival *L. plantarum* in simulated gastric fluid (SGF) and simulated intestinal fluid (SIF)

Probiotics were living microorganisms capable of providing beneficial effects or promoting health in the human body [8]. The probiotic bacterial strain used in this study was *Lactobacillus plantarum*, which was classified as a lactic acid bacterium and fell under the category of probiotic strains. Probiotic products could be utilized through microencapsulation of bacteria, which had been tested to enhance total probiotic bacteria when encapsulated in hydrocolloid beads (Table 2). The immobilization of probiotic bacteria was performed on the ulvan-alginate hydrogel, and the chosen treatment was ULV-ALG-a with a concentration of 1% ulvan and 2% alginate. Prior to application in the ULV-ALG-a treatment, the total probiotic bacteria were measured using UV-Vis spectrophotometry to determine the Optical Density (OD). The OD measurement of the probiotic bacteria intended for use in the ULV-ALG-a treatment was found to be 1.831. As the previous report by Oberoi [49] utilized 1.98 times the optical density (OD) when immobilizing *L. rhamnosus* in alginate beads, this initial OD value was adopted as the cell density for the targeted microencapsulated cells in ULV-ALG system. The viability of probiotic bacteria was tested under free encapsulated conditions and encapsulated within the hydrogel. The samples were subjected to three different time-based treatments, including immersion in a simulated gastric fluid (SGF) for 0, 60, and 120 minutes, followed by immersion in a simulated intestinal fluid (SIF).

Table 2 Probiotic survival *L. plantarum* in *simulated gastric fluid* (SGF) dan *simulated intestinal fluid* (SIF)

Survival of Probiotic ($\times 10^7$ log CFU/g)			
Simulation of gut	Time (h)	Free encapsulated	Encapsulated in ULV-ALG Hydrogel
SGF	0	130.54 ± 21.92	31.00 ± 9.89
	1	7.62 ± 0.11	6.15 ± 6.85
	2	<10	3.41 ± 3.80
SIF	3	-	0.42 ± 0.05
	4	-	0.14 ± 0.03

Table 2 presented the total lactic acid bacteria that grew in acidic and basic solutions. The viability of free cells drastically decreased within 2 hours, with the initial count of 130.54 x 10^7 log CFU/g reducing to <10 bacteria or too few to be counted due to the acidic effect of gastric fluid. Encapsulated bacteria, however, maintained their viability with an initial count of 31.00 x 10^7 log CFU/g, decreasing to 3.41 x 10^7 log CFU/g after 2 hours of immersion. The research results indicated that encapsulated bacteria exhibited higher viability than free cells in SGF solution. These findings aligned with report from Shi [50] who demonstrated that the use of polymers for probiotic encapsulation could protect and maintain probiotic viability under acidic conditions. The viability of free cells declined within 2 hours in SGF, making further immersion in SIF infeasible. In contrast, encapsulated bacteria managed to survive until SIF, with the initial count of 3.41 x 10^7 log CFU/g reducing to 0.14 x 10^7 log CFU/g after 2 hours of immersion. Although the viability of encapsulated *L. plantarum* bacteria decreased during SGF and SIF immersion, the observed decline was lower compared to free bacterial cells.

The viability of *Lactobacillus plantarum* bacteria in encapsulation was superior to free cells under both SGF and SIF conditions. This phenomenon could be attributed to alginates' stability in low-pH solutions while expanding in weakly basic conditions [51]. Ulvan also influenced these results, as it acted as a prebiotic, providing the necessary nutritional source to maintain the viability of probiotic bacteria [52]. Ulvan, derived from carbohydrates like polysaccharides found in *Ulva lactuca* seaweed, assisted in providing energy for the replication of probiotic bacteria. The dual function of ulvan-alginate as the main backbone in the hydrogel system not only supports the extracellular matrix condition of probiotic bacteria but also opens new avenues for further application, such as developing functional beverages loaded with these beads containing prebiotics and probiotics. This new system could potentially reinvent the form of probiotic drinks in the food and beverage industry.

4   Conclusions

The hydrogel beads based on ulvan-alginate obtained the selected formulation, namely ULV-ALG-a, with a composition of 1% ulvan and 2% alginate. The ULV-ALG-a formulation exhibited a superior shape compared to other formulations. These results were derived from the evaluation of gel fraction, swelling ratio, and rheology. The viability of *L. plantarum* bacteria using the ULV-ALG-a formulation with hydrogel encapsulation was proven to maintain bacterial viability under SGF and SIF conditions than the free encapsulated condition.

References

1.   F. Zendeboodi, N. Khorshidian, A. M. Mortazavian, and A. G. da Cruz, Curr. Opin. Food Sci. **32**, 103 (2020)
2.   T. Hernández-Barrueta, F. Martínez-Bustos, E. Castaño-Tostado, Y. Lee, M. J. Miller, and S. L. Amaya-Llano, LWT **124**, 109131 (2020)
3.   T. Tao, Z. Ding, D. Hou, S. Prakash, Y. Zhao, Z. Fan, D. Zhang, Z. Wang, M. Liu,

and J. Han, J. Food Eng. **252**, 10 (2019)

4. D. Y. Y. Tang, K. S. Khoo, K. W. Chew, Y. Tao, S.-H. Ho, and P. L. Show, Bioresour. Technol. **304**, 122997 (2020)

5. C. González-Ferrero, J. M. Irache, B. Marín-Calvo, L. Ortiz-Romero, R. Virto-Resano, and C. J. González-Navarro, J. Microencapsul. **37**, 242 (2020)

6. R. F. Trimudita and D. Djaenudin, J. Serambi Eng. **6**, 1832 (2021)

7. A. Terpou, A. Papadaki, I. Lappa, V. Kachrimanidou, L. Bosnea, and N. Kopsahelis, Nutrients **11**, 1591 (2019)

8. K. Papadimitriou, G. Zoumpopoulou, B. Foligné, V. Alexandraki, M. Kazou, B. Pot, and E. Tsakalidou, Front. Microbiol. **6**, (2015)

9. E. Vera-Pingitore, M. E. Jimenez, A. Dallagnol, C. Belfiore, C. Fontana, P. Fontana, A. von Wright, G. Vignolo, and C. Plumed-Ferrer, LWT - Food Sci. Technol. **71**, 288 (2016)

10. K. Abdul Khalil, Sci. Lett. **14**, 49 (2020)

11. S. Petraitytė and A. Šipailienė, LWT **110**, 307 (2019)

12. M. A. Gionet-Gonzales and J. K. Leach, Biomed. Mater. **13**, 034109 (2018)

13. A. Raise, S. Dupont, C. Iaconelli, C. Caliri, A. Charriau, P. Gervais, O. Chambin, and L. Beney, J. Drug Deliv. Sci. Technol. **56**, 101608 (2020)

14. K. Sultana, G. Godward, N. Reynolds, R. Arumugaswamy, P. Peiris, and K. Kailasapathy, Int. J. Food Microbiol. **62**, 47 (2000)

15. W. Li, L. Liu, H. Tian, X. Luo, and S. Liu, Carbohydr. Polym. **223**, 115065 (2019)

16. A. J. Priya, S. P. Vijayalakshmi, and A. M. Raichur, J. Agric. Food Chem. **59**, 11838 (2011)

17. P. E. Ramos, M. A. Cerqueira, J. A. Teixeira, and A. A. Vicente, Crit. Rev. Food Sci. Nutr. **58**, 1864 (2018)

18. L. T. Hansen, P. . Allan-Wojtas, Y.-L. Jin, and A. . Paulson, Food Microbiol. **19**, 35 (2002)

19. Q. Yang, J. Peng, H. Xiao, X. Xu, and Z. Qian, Carbohydr. Polym. **278**, 118952 (2022)

20. W. Ramadhan, G. Kagawa, Y. Hamada, K. Moriyama, R. Wakabayashi, K. Minamihata, M. Goto, and N. Kamiya, ACS Appl. Bio Mater. **2**, 2600 (2019)

21. R. Wakabayashi, W. Ramadhan, K. Moriyama, M. Goto, and N. Kamiya, Polym. J. (2020)

22. W. Ramadhan, G. Kagawa, K. Moriyama, and R. Wakabayashi, Sci. Rep. **10**, 1 (2020)

23. W. Ramadhan, Y. Ohama, K. Minamihata, K. Moriyama, R. Wakabayashi, M. Goto, and N. Kamiya, J. Biosci. Bioeng. **130**, 416 (2020)

24. R. Wakabayashi, R. Ishiyama, N. Kamiya, and M. Goto, Medchemcomm **5**, 1515 (2014)

25. K. Minamihata, Y. Hamada, G. Kagawa, W. Ramadhan, A. Higuchi, K. Moriyama, R. Wakabayashi, M. Goto, and N. Kamiya, ACS Appl. Bio Mater. **3**, 7734 (2020)

26. Y. Hao, W. Zhao, L. Zhang, X. Zeng, Z. Sun, D. Zhang, P. Shen, Z. Li, Y. Han, P. Li, and Q. Zhou, Mater. Des. **193**, 108863 (2020)

27. B. U. Putra, S. D. Hardiningtyas, N. Hastuti, W. Ramadhan, Uju, M. A. Razi, and L. Agustini, Mater. Today Commun. 108248 (2024)

28. R. Gheorghita Puscaselu, A. Lobiuc, M. Dimian, and M. Covasa, Polymers (Basel). **12**, 2417 (2020)

29. S. M. Pradana, Arena Tekst. **36**, (2021)

30. S. Asadi, S. Eris, and S. Azizian, ACS Omega **3**, 15140 (2018)

31. N. Selvasudha, R. Goswami, M. Tamil Mani Subi, S. Rajesh, K. Kishore, and H. R. Vasanthi, Carbohydr. Polym. Technol. Appl. **6**, 100342 (2023)

32. J. T. Kidgell, M. Magnusson, R. de Nys, and C. R. K. Glasson, Algal Res. **39**, 101422 (2019)

33. M. N. Abrar, S. D. Hardiningtyas, W. Ramadhan, R. Wakabayashi, B. U. Putra, and Uju, Squalen Bull. Mar. Fish. Postharvest Biotechnol. **18**, 129 (2023)

34. W. Ramadhan, U. Uju, S. D. Hardiningtyas, R. F. Pari, N. Nurhayati, and D. Sevica, J. Pengolah. Has. Perikan. Indones. **25**, 132 (2022)

35. E. Sulastri, R. Lesmana, M. S. Zubair, K. M. Elamin, and N. Wathoni, Chem. Pharm. Bull. **69**, 432 (2021)

36. X. Zhao, Q. Lang, L. Yildirimer, Z. Y. Lin, W. Cui, N. Annabi, K. W. Ng, M. R. Dokmeci, A. M. Ghaemmaghami, and A. Khademhosseini, Adv. Healthc. Mater. **5**, 108 (2016)

37. [AOAC] Association of Official Analytical Chemists, *Official Methods of Analysis of AOAC International (17th Ed.)*, 17th ed. (AOAC International Press, Maryland, 2000)

38. M. Afzaal, A. U. Khan, F. Saeed, M. S. Arshad, M. A. Khan, M. Saeed, A. A. Maan, M. K. Khan, Z. Ismail, A. Ahmed, T. Tufail, H. Ateeq, and F. M. Anjum, Food Sci. Nutr. **8**, 1649 (2020)

39. H. Dominguez and E. P. Loret, Mar. Drugs **17**, 1 (2019)

40. J. Venkatesan, B. Lowe, S. Anil, P. Manivasagan, A. A. Al Kheraif, K. Kang, and S. Kim, Starch - Stärke **67**, 381 (2015)

41. E. Hernández-Garibay, J. A. Zertuche-González, and I. Pacheco-Ruíz, J. Appl. Phycol. **23**, 537 (2011)

42. N. Wahlström, F. Nylander, E. Malmhäll-Bah, K. Sjövold, U. Edlund, G. Westman, and E. Albers, Carbohydr. Polym. **233**, 115852 (2020)

43. L. Cunha and A. Grenha, Mar. Drugs **14**, 42 (2016)

44. R. Wakabayashi, W. Ramadhan, K. Moriyama, M. Goto, and N. Kamiya, Polym. J. **52**, 899 (2020)

45. M. Gomez-Florit, A. Pardo, R. M. A. Domingues, A. L. Graça, P. S. Babo, R. L. Reis, and M. E. Gomes, Molecules **25**, 1 (2020)

46. Lh. Yahia, J. Biomed. Sci. **04**, 1 (2015)

47. G. Kimbell and M. A. Azad, in *Bioinspired Biomim. Mater. Drug Deliv.* (Elsevier, 2021), pp. 295–318

48. A. Dsouza, C. Constantinidou, T. N. Arvanitis, D. M. Haddleton, J. Charmet, and R. A. Hand, ACS Appl. Mater. Interfaces **14**, 47323 (2022)

49. K. Oberoi, A. Tolun, Z. Altintas, and S. Sharma, Foods **10**, 1999 (2021)

50. L.-E. Shi, Z.-H. Li, D.-T. Li, M. Xu, H.-Y. Chen, Z.-L. Zhang, and Z.-X. Tang, J. Food Eng. **117**, 99 (2013)

51. H. Gandomi, S. Abbaszadeh, A. Misaghi, S. Bokaie, and N. Noori, LWT - Food Sci. Technol. **69**, 365 (2016)

52. S. Shalaby M and H. Amin H, J. Probiotics Heal. **07**, (2019)